PROCEEDINGS of the
23rd International Congress on Acoustics

9 to 13 September 2019 in Aachen, Germany

Study on the sound transmission loss of a truncated conical shell excited by an incident plane acoustic wave

Masoud GOLZARI[1]; Ali Asghar JAFARI[2]

[1] K.N. Toosi University of Technology, Iran

[2] K.N. Toosi University of Technology, Iran

ABSTRACT

In this paper, a theoretical model is proposed to study on the sound transmission loss of a thin-walled truncated circular conical shell subjected to an incident plane acoustic wave. The shell motion is governed by Love's theory and a convergent power series solution is used to obtain exact displacements of the shell. The current results are firstly validated against those of the experimental and analytical works reported in the literature. Parametric study is then conducted to investigate the effects of several important design parameters including different boundary conditions at the ends of the shell, cone angle, incidence sound wave angle, wall thickness and material properties of the shell on the characteristics of the sound transmission loss. The presented model can be useful and effective in the acoustic design stage of the truncated conical shells.

Keywords: Sound transmission loss, Truncated Conical Shell, Plane sound wave

1. INTRODUCTION

Plates and shells are widely applied in many types of industries such as aerospace, automotive, marine and military. The interaction of these structures and surrounding fluids mostly induces transmission of undesirable vibroacoustic energy, which can lead to structural fatigue and noise pollution in the systems. For instance, the transmission of sound power into the vehicle body such as aircraft, train and car can be a discomfort for the passengers. Therefore, the acoustic transmission problem of plates and shells has attracted extensive research attention and numerous works on the transmission of sound through panels and cylindrical shells have been performed for decades.

The early study for calculating the sound transmission through panel structures can be traced back to the work carried out by Beranek and Work (1). Koval (2) studied the sound transmission loss of aircraft fuselage panels and the influences of panel curvature, fuselage pressurization and external air flow on the acoustic behavior of the structure. Lee and Kim (3) developed a theoretical model to investigate on the sound transmission characteristics of a thin plate stiffened by equally spaced line stiffeners. Xin et al. (4, 5) theoretically and experimentally obtained the transmission loss of thin double-panel partitions with finite dimensions. They showed that the effect of boundary conditions is more considerable at low frequencies. The transmission loss of triple-panel structures lined with porous layers was studied by Liu (6). Mana and Sonti (7) presented a theoretical model to compute the acoustic transmission through a finite perforated panel set. Qiao et al. (8) studied on the sound insulation of a periodically rib-stiffened double panel with porous lining.

The prediction of the acoustic transmission through thin-walled cylindrical shells was firstly performed by Smith (9). For an aircraft fuselage, Koval analytically studied the sound transmission into a thin cylindrical shell under flight conditions (10) an orthotropic shell (11), and a laminated composite cylindrical shell (12). Lee and Kim (13, 14) carried out analytical and experimental analyses for the transmission loss of thin single- and double-walled cylindrical shells. The influences of geometrical and mechanical properties of the shells were also explored by them. Zhou et al. (15) analytically investigated on the transmission loss of sandwich cylindrical shells with infinite length. Magniez et al. (16) proposed an analytical model for calculating the sound transmission loss of orthotropic sandwich cylindrical shells lined with porous layer. Golzari and Jafari (17) studied on the

[1] mgolzari@mail.kntu.ac.ir
[2] ajafari@kntu.ac.ir

sound insulation performance of triple- and multi-walled sandwich cylindrical shell with poroelastic layers and air gaps in a diffuse sound field.

Conical shells are extensively used in many practical applications such as aircrafts, submarines, rockets, and tanks. However, study on the sound transmission behavior of these highly complicated structures has received a little attention for decades. In this regard, it can be referred to the work experimentally performed by Vipperman et al. (18) who measured the acoustic transmission through a truncated conical shell. Therefore, the main purpose of this study is to propose a theoretical model for investigating on the sound transmission through truncated circular conical shells and the influences of different boundary conditions at the ends of the shell, cone angle, incidence sound wave angle, thickness and material properties of the shell on the transmission loss characteristics.

2. FORMULATION OF THE VIBROACOUSTIC PROBLEM

The geometry and coordinate system of a truncated circular conical shell considered in this study are shown in Figure 1. R_1 and R_2 are the radiuses at the smaller and larger ends, respectively, α is the semi-vertex angle, L is the height, L_s is the slant height, and h is the wall thickness. The boundary conditions at the ends of the thin isotropic shell are simply supported. In the curvilinear coordinate system, the x and θ respectively show the meridional and circumferential directions, and z is normal to the shell surface. A harmonic plane acoustic wave impinges on the external surface with the incidence angle β with respect to N, and it is partially transmitted into the inner cavity, which is assumed with no reverberation.

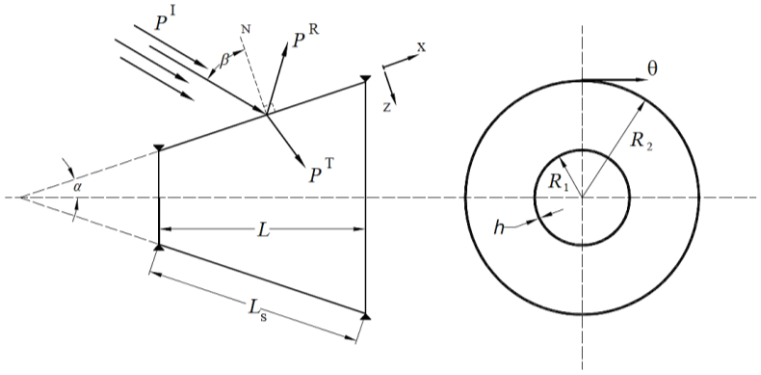

Figure 1 – A schematic sketch of the sound transmission through the truncated conical shell

The equations of motion of the thin-walled truncated conical shell based on Love's shell theory are written as follows (19):

$$L_1\{u,v,w\} = \rho_s h \frac{\partial^2 u}{\partial t^2} \tag{1}$$

$$L_2\{u,v,w\} = \rho_s h \frac{\partial^2 v}{\partial t^2} \tag{2}$$

$$L_3\{u,v,w\} + \Delta P = \rho_s h \frac{\partial^2 w}{\partial t^2} \tag{3}$$

where u, v and w are, respectively, the displacement components at the neutral surface in x, θ and z directions. ρ_s is the material density of the conical shell. The expression $\Delta P = (P^I + P^R) - P^T$ denotes the pressure difference applying on the shell, in which P^{I}, P^{R} and P^{T} are the incident, reflected and transmitted sound pressures, respectively. The partial differential operators L_1, L_2 and L_3 are also given in Appendix.

As shown in Figure 2, to determine the acoustic pressures at the shell and fluid media interfaces, the conical shell is divided into N parts which are narrow enough to be considered locally cylindrical, in which the quantity of the sound pressures on the conical segment equals that on the equivalent cylindrical counterpart with the same mean radius $R_{0,i}$ and length l_i. Hence the pressure waves in the cylindrical coordinate system can be written as (15, 17):

$$P_i^I(r,\theta,X,t) = \sum_{n=0}^{\infty} p^I \varepsilon_n (-j)^n J_n(k_{1r} r)\, cos(n\theta) \exp[j(\omega t - k_{1X}(X_i + X)] \tag{4}$$

$$P_i^{\mathrm{R}}(r,\theta,X,t) = \sum_{n=0}^{\infty} p_{n,i}^{\mathrm{R}} H_n^2(k_{2r} r) \cos(n\theta) \exp[\mathrm{j}(\omega t - k_{2X} X)] \tag{5}$$

$$P_i^{\mathrm{T}}(r,\theta,X,t)=\sum_{n=0}^{\infty}p_{n,i}^{\mathrm{T}}H_n^1(k_{3r}r)\cos(n\theta)\exp[\mathrm{j}(\omega t-k_{3X}X)],\quad i=1,2,..,N \tag{6}$$

where p^{I}, p^{R} and p^{T} are the amplitudes of the incident, reflected and transmitted sound waves, respectively. r, θ and capital letter X are, respectively, the radial, circumferential and axial directions in the cylindrical coordinate system. ω is the angular frequency of the incident sound wave, $\mathrm{j}=\sqrt{-1}$, n is the circumferential mode number, ε_n is the Neumann factor in which ε_n=1 for n=0 and ε_n=2 for n=1,2,… . J_n, H_n^1 and H_n^2 are the Bessel function of the first kind, Hankel function of the first kind and Hankel function of the second kind of order n, respectively. Since the travelling waves within the system are driven by the incident wave, the axial wavenumbers in the fluid media must be equal, i.e. $k_{1X}=k_{2X}=k_{3X}$. Also $k_{1X}=k_1\sin(\alpha+\beta)$ and $k_{1r}=k_1\cos(\alpha+\beta)$, in which $k_1=\omega/c$. c is the speed of sound in the fluid media.

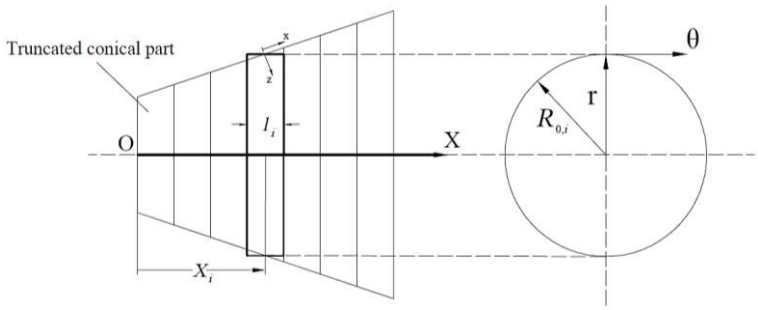

Figure 2 – A schematic sketch showing the narrow conical segments

The truncated conical segments in Figure 2 are connected together by using eight continuity equations at each intersection. These boundary conditions can be formulated as follows:

$$u_i\big|_{x=\frac{l_{s,i}}{2}}=u_{i+1}\big|_{x=-\frac{l_{s,i+1}}{2}},\qquad v_i\big|_{x=\frac{l_{s,i}}{2}}=v_{i+1}\big|_{x=-\frac{l_{s,i+1}}{2}},\qquad w_i\big|_{x=\frac{l_{s,i}}{2}}=w_{i+1}\big|_{x=-\frac{l_{s,i+1}}{2}} \tag{7}$$

$$\frac{\partial w_i}{\partial x}\Big|_{x=\frac{l_{s,i}}{2}}=\frac{\partial w_{i+1}}{\partial x}\Big|_{x=-\frac{l_{s,i+1}}{2}},\qquad N_{xx,i}\big|_{x=\frac{l_{s,i}}{2}}=N_{xx,i+1}\big|_{x=-\frac{l_{s,i+1}}{2}},\qquad N_{x\theta,i}\big|_{x=\frac{l_{s,i}}{2}}=N_{x\theta,i+1}\big|_{x=-\frac{l_{s,i+1}}{2}} \tag{8}$$

$$M_{xx,i}\big|_{x=\frac{l_{s,i}}{2}}=M_{xx,i+1}\big|_{x=-\frac{l_{s,i+1}}{2}},\qquad V_{xz,i}\big|_{x=\frac{l_{s,i}}{2}}=V_{xz,i+1}\big|_{x=-\frac{l_{s,i+1}}{2}}\quad \text{where: } V_{xz}=Q_{xz}+\frac{1}{R(x)}\frac{\partial M_{x\theta}}{\partial\theta} \tag{9}$$

where i=1,2,..,N-1, $l_{s,i}$ is the slant length of the ith cone and $R(x)=R_0+x\sin\alpha$.

At the interfaces between the truncated conical segments and the fluid media, the particle velocities of the fluid media in the z direction normal to the shell surface must equal to the normal velocity of the shell. Hence, the following relations are obtained:

$$\left(V_{r,i}^{\mathrm{I}}+V_{r,i}^{\mathrm{R}}\right)\cos\alpha+\left(V_{X,i}^{\mathrm{I}}+V_{X,i}^{\mathrm{R}}\right)\sin\alpha=\frac{\partial w_i}{\partial t} \tag{10a}$$

$$V_{r,i}^{\mathrm{T}}\cos\alpha+V_{X,i}^{\mathrm{T}}\sin\alpha=\frac{\partial w_i}{\partial t} \tag{10b}$$

where V_{r} and V_{X} are the sound particle velocities in the radial and longitudinal directions of the cylindrical coordinate system, respectively.

The boundary conditions at the ends of the truncated conical shell, i.e. x=0,L_{s}, for the simply supported (S), clamped (C) and free (F) boundary conditions are defined in equations (11)-(13), respectively, as follows:

$$v=0,\qquad w=0,\qquad N_{xx}=0,\qquad M_{xx}=0 \tag{11}$$

$$u=0,\qquad v=0,\qquad w=0,\qquad \frac{\partial w}{\partial t}=0 \tag{12}$$

$$N_{xx}=0,\qquad N_{x\theta}=0,\qquad M_{xx}=0,\qquad V_{xz}=0 \tag{13}$$

General solution in the form of power series for the displacement components of the each truncated conical part can be expressed as:

$$u(x,\theta,t)=\sum_{n=0}^{\infty}U(x)\cos(n\theta)\exp(\mathrm{j}\omega t)\quad \text{where:}\quad U(x)=\sum_{m=0}^{\infty}a_m x^m \tag{14}$$

$$v(x,\theta,t)=\sum_{n=0}^{\infty}V(x)\cos(n\theta)\exp(\mathrm{j}\omega t)\quad \text{where:}\quad V(x)=\sum_{m=0}^{\infty}b_m x^m \tag{15}$$

$$w(x,\theta,t)=\sum_{n=0}^{\infty}W(x)\cos(n\theta)\exp(\mathrm{j}\omega t)\quad\text{where:}\quad W(x)=\sum_{m=0}^{\infty}c_m x^m \tag{16}$$

in which a_{m}, b_{m} and c_{m} are the constants.

By using equations 4-6, 10 and 14-16, and substituting them into the governing equations given in equations 1-3, it is found that the displacements of the conical parts can be obtained in terms of eight unknown constants a_0, a_1, b_0, b_1, c_0, c_1, c_2 and c_3 as follows:

$$\begin{bmatrix}U(x)\\V(x)\\W(x)\end{bmatrix}=\begin{bmatrix}u_1(x) & \cdots & u_8(x)\\v_1(x) & \cdots & v_8(x)\\w_1(x) & \cdots & w_8(x)\end{bmatrix}\mathbf{x}+\begin{bmatrix}u_0(x)\\v_0(x)\\w_0(x)\end{bmatrix} \tag{17}$$

where $u_{p,i}(x)$, $v_{p,i}(x)$ and $w_{p,i}(x)$ (p=0,1,2,…,8; i=1,2,…,N) are the base functions and $\mathbf{x}=[a_0\ a_1\ b_0\ b_1\ c_0\ c_1\ c_2\ c_3]^{\mathrm{T}}$.

Substituting equation 17 into the boundary conditions at the intersections between the conical strips provided in equations 7-9 and the boundary conditions at both ends of the truncated conical shell, here simply supported boundary condition in equation 11, leads to the following matrix equation for each circumferential mode number n:

$$\mathbf{Ax}=\mathbf{b} \tag{18}$$

By solving the matrix equation 18, the displacement components of the truncated conical shell are determined, which are used to obtain the reflected and transmitted sound pressures from equations 10.

Finally, the transmission loss is defined in below (14, 15):

$$\mathrm{TL}=-10\log\frac{\sum_{n=0}^{\infty}W_n^{\mathrm{T}}}{W^{\mathrm{I}}} \tag{19}$$

where the incident sound power W^{I} and the transmitted sound power $W_n{}^{\mathrm{T}}$ are:

$$W^{\mathrm{I}}=\frac{1}{2}\mathrm{Re}\left\{\int P^{\mathrm{I}}(V^{\mathrm{I}})^{*}dS_{\mathrm{in}}\right\} \tag{20}$$

$$W_n^{\mathrm{T}}=\frac{1}{2}\mathrm{Re}\left\{\int P^{\mathrm{T}}\left(\frac{\partial w}{\partial t}\right)^{*}dS_{\mathrm{ou}}\right\} \tag{21}$$

where Re $\{\cdot\}$ and $(*)$ represent the real part and complex conjugate of the argument, respectively. S_{in} is the plane projection of the conical shell surface and $dS_{ou}=(R_0+x\sin\alpha)dxd\theta$. $V^{\mathrm{I}}=P^{\mathrm{I}}/\rho_{\mathrm{I}}c_{\mathrm{I}}$ is the particle velocity of the incident plane sound wave, in which ρ_{I} is the density of external fluid. In a randomly incidence field, the average transmission loss is also defined by (14):

$$\mathrm{TL}_{\mathrm{av}}=-10\log\left[2\int_0^{\beta_{\mathrm{lim}}}\left(\frac{\sum_{n=0}^{\infty}W_n^{\mathrm{T}}}{W^{\mathrm{I}}}\right)\sin\beta\cos\beta d\beta\right] \tag{22}$$

where β_{lim} is the limiting angle of incident sound wave, in which above this angle it is assumed that no acoustic wave can cross the conical shell.

3. RESULTS AND DISCUSSION

In Table 1, the basic property parameters of the truncated conical steel shell are presented. The boundary conditions at the ends of the shell are simply supported. The amplitude of the incident acoustic wave is 1 Pa, and the fluid media in the outside and inside of the shell is ambient air at 20°C with the density of 1.21 kg m^{-3} and the sound speed of 343.2 m s^{-1}.

3.1 Convergence checking

Because the acoustic waves, displacement components and transmission loss are expressed as series form, the use of inadequate number of circumferential modes n leads to unreliable outcomes. Therefore, the convergence checking should be carried out during the analysis. Figure 3 shows the variation of transmission loss with the circumferential mode number n at the frequencies of 200 Hz, 2 kHz and 20 kHz. The mode convergence curve changes with n until it reaches a constant value. It is also observed that the number of modes needed for converging increases as the frequency is enhanced.

3.2 Model validation

Since the acoustic transmission through conical shells has seldom been studied as mentioned in Section 1, Figures 4 and 5 respectively show the comparisons carried out between the current results and those of Zhou et al. (15), and Lee and Kim (14) for circular cylindrical shells. It should be noted that the sound transmission problem of the cylindrical shells can be achieved by substituting α=0 into the governing equations implemented for the truncated conical shells in Section 2. From these figures,

Table 1 – Property parameters of the truncated conical steel shell

Symbol	Description	Value
ρ_s	Material density	7850 kg m^{-3}
E	Young's modulus of elasticity	2×10^{11} Pa
μ	Poisson's ratio	0.3
R_1	Small radius	0.1 m
R_2	Large radius	0.144 m
α	Semi-vertex angle	5°
h	Thickness	1 mm
L	Height	0.5 m

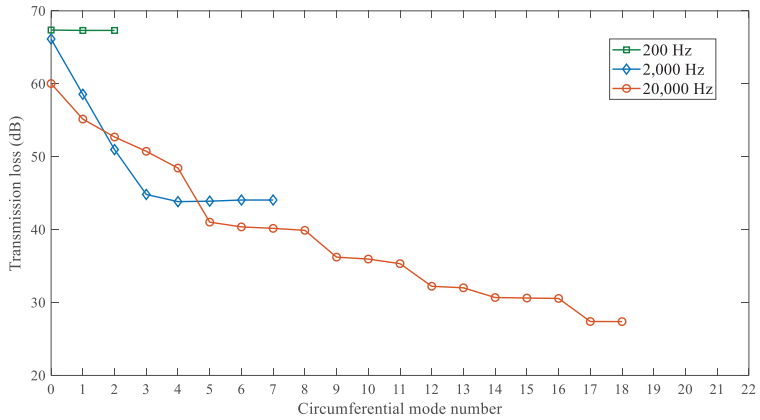

Figure 3 – Convergence checking for the sound transmission loss of the truncated conical shell

it is observed that the results of the present model are in a good agreement with those of Zhou et al. (15) and Lee and Kim (14) at middle and high frequencies. However, discrepancies particularly in the low frequency range can be attributed to two main reasons: (a) because the analytical models proposed by Zhou and Lee are presented for the shell with infinite length, they are not capable to take into account the effects of the finite-size assumptions such as the implication of boundary constraints at the ends. Considering the boundary condition increases the shell stiffness which leads to an improvement in the transmission loss outcomes at low frequencies. However, by increasing of the length size, the analytical predictions approach each other at these frequencies. (b) In the Lee's experimental setting the creation of an incident plane acoustic wave condition by a single external sound source and the acoustic room without reverberation is not clear. Also, the inner cavity in the current model is assumed to be anechoic while in the experimental model is reverberant.

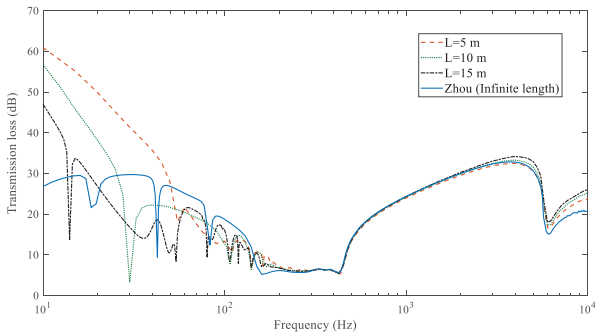

Figure 4 – Comparison of the present results with the analytical results of Zhou et al. (15), β=45°

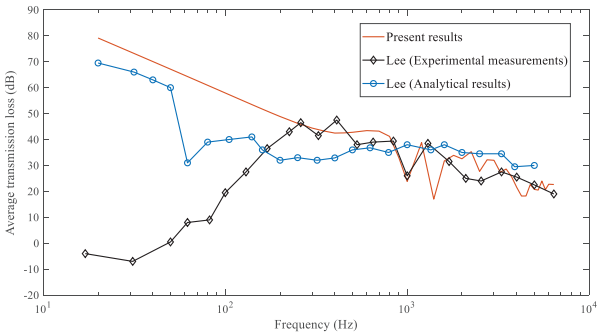

Figure 5 – Comparison of the present results with the experimental measurements and analytical results of Lee and Kim (14)

3.3 Parametric study

In Figure 6, the transmission loss outcomes of the truncated conical shell with free-free (F-F), simply-simply (S-S) and clamped-clamped (C-C) boundary conditions are presented. It can be seen that the effect of boundary constraint through changing the shell stiffness is more considerable at the frequencies below 1000 Hz. The highest and lowest transmission loss amplitude are generally predicted by the fully clamped and free boundary conditions, respectively. However by disappearing the influence of the boundary conditions, there is no significant behavior for the sound transmission losses at higher frequencies and the tendency of the curves is similar.

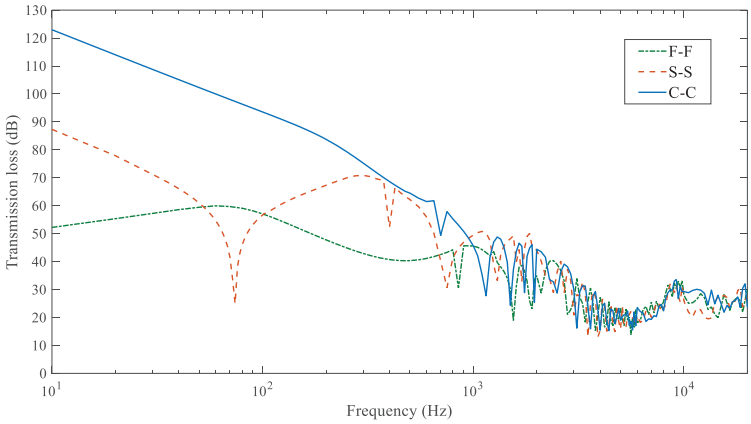

Figure 6 – Effect of the boundary conditions on the transmission loss of the truncated conical shell, β=45°

Figure 7 shows the transmission loss of the truncated conical shell at different semi-vertex angles α=0°, 5°, 10°. It should be noted that α=0° is corresponded with the cylindrical shell with the mean radius 0.122 m, which equals to the mean radius of the conical shell with the parameters given in Table 1. It is concluded that the transmission loss at frequencies below 400 Hz is reduced as the cone angle increases, specifically for the cylindrical shell compared with the conical shell. This can be caused by reducing the shell stiffness when the cone angle is enhanced. The mass law states that the sound transmission loss increases with the mass or frequency and decreases by the acoustic impedance of the fluid media (17). Therefore, increasing of the cone angle leads to slightly superior transmission loss at higher frequencies as a result of the mass increase.

Figure 8 represents the acoustic transmission of the truncated conical shell at different incidence angles. The transmission of sound into the shell is significantly increased in the frequency range 250 Hz to 2800 Hz as the incidence angle decreases. However, an improvement in the transmission loss is observed at other frequencies.

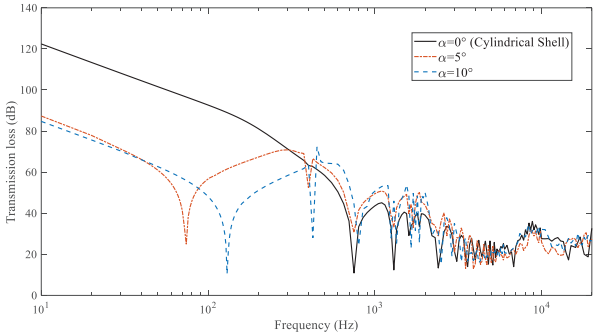

Figure 7 – Effect of the cone angle on the transmission loss of the truncated conical shell, R_1=0.1 m, L=0.5 m, β=45°

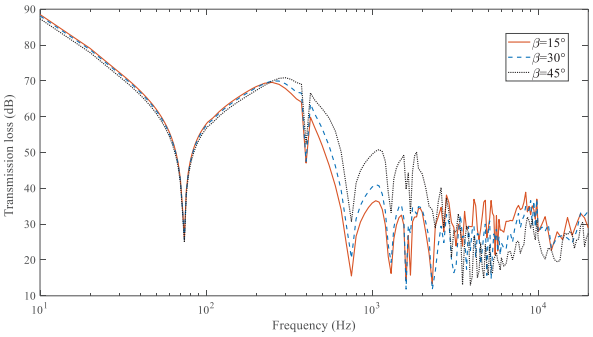

Figure 8 – Effect of the incidence acoustic wave angle on the transmission loss of the truncated conical shell

Figure 9 illustrates the effect of the shell thickness on the transmission loss of the truncated conical shell. By increasing of the thickness, the transmission of sound into the inner cavity is reduced over a wide frequency range. This is because both the shell stiffness and shell mass enhance. However, it should be noted that an enhancement in the shell thickness is not always an appropriate perspective to reach superior sound insulation performance because of the design restriction in the weight, construction procedure and costs.

A comparison between the transmission loss outcomes for three types of materials including aluminum (with density 2700 kg m^{-3}, Young modulus 69 GPa and Poisson's ratio 0.33), steel and brass (with density 8553 kg m^{-3}, Young modulus 104 GPa and Poisson's ratio 0.37) is carried out in Figure 10. It is shown that the best transmission loss at low and middle frequencies is achieve by the conical steel shell, whereas the conical shell made of brass has the highest amplitude of the transmission loss at high frequencies. Because steel and brass have the most stiffness and mass, respectively.

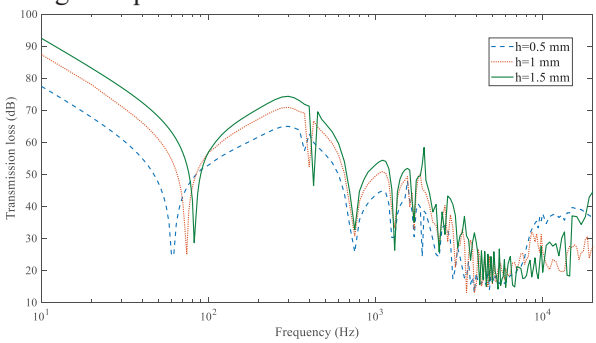

Figure 9 – Effect of the shell thickness on the the transmission loss of the truncated conical shell, β=45°

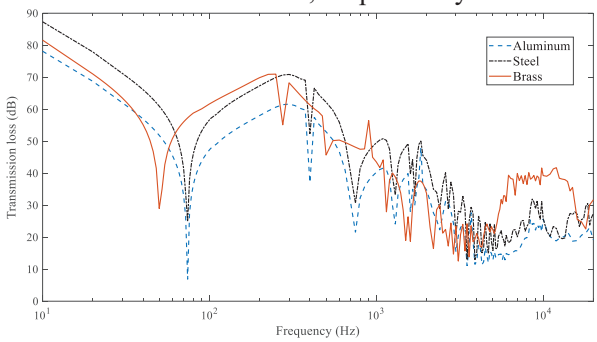

Figure 10 – Effect of the shell material properties on the transmission loss of the truncated conical shell. β=45°

4. CONCLUSIONS

Sound transmission loss of a thin-walled truncated circular conical shell, which is excited by an oblique incident plane sound wave, was theoretically investigated. Love's theory was used to implement the governing equations of the shell motion and a convergent power series solution was employed to obtain the exact displacements of the conical shell. In order to compute the acoustic pressure loadings at the structure-fluid interfaces, the shell is divided into segments which are narrow enough to be taken into account locally cylindrical. At first, the model predictions were validated against both their experimental and analytical counterparts provided in previous studies and in this regard, a good agreement was achieved. Then, the effects of several key parameters were investigated on the transmission loss, which can be summarized as follows:

The effect of the boundary constraint is found to be more significant at low frequencies. In this regard, the comparison between the results of simply supported-simply supported, clamped-clamped and free-free boundary conditions shows the highest and lowest transmission loss for the fully clamped boundary condition and free boundary condition, respectively. However, a similar trend for the transmission loss behaviors is observed at higher frequencies.

The transmission loss is reduced in the low frequency range as the cone angle increases. However, an enhancement in the amplitude of the transmission loss is observed in the middle and high frequency bands with a rise in the vertex angle of conical shell.

Increasing of the shell thickness results in better noise insulation performance in almost the entire frequency spectrum.

It is found that the transmitted sound power increases at middle frequencies when the incidence angle decreases, which is opposite to low and high frequencies.

Also, the comparison of the transmission loss results of the conical shell with different types of materials including brass, steel and aluminum represents superior sound insulation ability for steel at low and middle frequencies, whereas brass has better performance in the high frequency range.

The proposed model can be considered as an effective tool in the acoustic design of the truncated conical shells.

APPENDIX

The partial differential operators given in equations 1 to 3 are:

$$L_1\{u,v,w\} = C\frac{\partial^2 u}{\partial x^2} + \frac{C(1-\mu)}{2R_{(x)}^2}\frac{\partial^2 u}{\partial \theta^2} + \frac{C\sin\alpha}{R_{(x)}}\frac{\partial u}{\partial x} - \frac{C\sin^2\alpha}{R_{(x)}^2}u + \frac{C(1+\mu)}{2R_{(x)}}\frac{\partial^2 v}{\partial x \partial \theta} \\ \frac{C(\mu-3)\sin\alpha}{2R_{(x)}^2}\frac{\partial v}{\partial \theta} + \frac{C\mu\cos\alpha}{R_{(x)}}\frac{\partial w}{\partial x} - \frac{C\sin\alpha\cos\alpha}{R_{(x)}^2}w \qquad \text{(A1)}$$

$$L_2\{u,v,w\} = \frac{C(1+\mu)}{2R_{(x)}}\frac{\partial^2 u}{\partial x\partial\theta} + \frac{C(3-\mu)\sin\alpha}{2R_{(x)}^2}\frac{\partial u}{\partial\theta} + \left(\frac{C(1-\mu)}{2} + \frac{D(1-\mu)\cos^2\alpha}{2R_{(x)}^2}\right)\frac{\partial^2 v}{\partial x^2}$$
$$\left(\frac{C}{R_{(x)}^2} + \frac{D\cos^2\alpha}{R_{(x)}^4}\right)\frac{\partial^2 v}{\partial\theta^2} + \left(\frac{C(1-\mu)\sin\alpha}{2R_{(x)}} - \frac{D(1-\mu)\cos^2\alpha\sin\alpha}{2R_{(x)}^3}\right)\frac{\partial^2 v}{\partial\theta^2} - \frac{C(1-\mu)\sin^2\alpha}{2R_{(x)}^2}v$$
$$-\frac{D\cos\alpha}{R_{(x)}^4}\frac{\partial^3 w}{\partial\theta^3} - \frac{D\cos\alpha}{R_{(x)}^2}\frac{\partial^3 w}{\partial x^2\partial\theta} - \frac{D\sin\alpha\cos\alpha}{R_{(x)}^3}\frac{\partial^2 w}{\partial x\partial\theta} + \frac{C\cos\alpha}{R_{(x)}^2}\frac{\partial w}{\partial\theta} \quad \text{(A2)}$$

$$L_3\{u,v,w\} = -\frac{C\mu\cos\alpha}{R_{(x)}}\frac{\partial u}{\partial x} - \frac{C\cos\alpha\sin\alpha}{R_{(x)}^2}u - D\frac{\partial^4 w}{\partial x^4} - \frac{2D\sin\alpha}{R_{(x)}}\frac{\partial^3 w}{\partial x^3} + \frac{D\sin^2\alpha}{R_{(x)}^2}\frac{\partial^2 w}{\partial x^2} - \frac{D\sin^3\alpha}{R_{(x)}^3}\frac{\partial w}{\partial x}$$
$$-\frac{D}{R_{(x)}^4}\frac{\partial^4 w}{\partial\theta^4} - \frac{4D\sin^2\alpha}{R_{(x)}^4}\frac{\partial^2 w}{\partial\theta^2} + \left(\frac{4D\sin^2\alpha\cos\alpha}{R_{(x)}^4} - \frac{C\cos\alpha}{R_{(x)}^2}\right)\frac{\partial v}{\partial\theta} - \frac{2D}{R_{(x)}^2}\frac{\partial^4 w}{\partial x^2\partial\theta^2} - \frac{C\cos^2\alpha}{R_{(x)}^2}w$$
$$\frac{2D\sin\alpha}{R_{(x)}^3}\frac{\partial^3 w}{\partial x\partial\theta^2} + \frac{D\cos\alpha}{R_{(x)}^4}\frac{\partial^3 v}{\partial\theta^3} - \frac{3D\sin\alpha\cos\alpha}{R_{(x)}^3}\frac{\partial^2 v}{\partial x\partial\theta} + \frac{D\cos\alpha}{R_{(x)}^2}\frac{\partial^3 v}{\partial x^2\partial\theta} \quad \text{(A3)}$$

where $C = Eh/(1-\mu^2)$ and $D = Eh^3/12(1-\mu^2)$ are the membrane stiffness and the bending stiffness of the truncated conical shell, respectively, in which E is the Young's modulus and μ is the Poisson's ratio of the shell.

REFERENCES

1. Beranek LL, Work GA. Sound transmission through multiple structures containing flexible blankets. J Acoust Soc Am 1949;21:419-428.
2. Koval LR. Effect of airflow, panel curvature, and internal pressurization on field-incidence transmission loss. J Acoust Soc Am 1976;59:1379–1385.
3. Lee JH, Kim J. Analysis of sound transmission through periodically stiffened panels by space-harmonic expansion method. J Sound Vib 2002;251:349-366.
4. Xin FX, Lu TJ, Chen CQ. Vibroacoustic behavior of clamp mounted double-panel partition with enclosure air cavity. J Acoust Soc Am 2008;124:3604-3612.
5. Xin FX, Lu TJ. Analytical and experimental investigation on transmission loss of clamped double panels: Implication of boundary effects. J Acoust Soc Am 2009;125:1506-1517.
6. Liu Y. Sound transmission through triple-panel structures lined with poroelastic materials. J Sound Vib 2015;339:376-395.
7. Mana AA, Sonti VR. Sound transmission through a finite perforated panel set in a rigid baffle: A fully coupled analysis. J Sound Vib 2018;414:126-156.
8. Qiao H, He Z, Jiang W, Peng W. Sound transmission of periodic composite structure lined with porous core: Rib-stiffened double panel set. J Sound Vib 2019;440:256-276.
9. Smith JPW. Sound transmission through thin cylindrical shells. J Acoust Soc Am 1957;29:721-729.
10. Koval LR. On sound transmission into a thin cylindrical shell under "flight Conditions", J. Sound Vib. 48 (1976) 265-275.
11. Koval LR. On sound transmission into an orthotropic shell. J Sound Vib 1979;63:51-59.
12. Koval LR. Sound transmission into a laminated composite cylindrical shell. J Sound Vib 1980;71:523-530.
13. Lee JH, Kim J. Analysis and measurement of sound transmission through a double-walled cylindrical shell. J Sound Vib 2002;251:631-649.
14. Lee JH, Kim J. Study on sound transmission characteristics of a cylindrical shell using analytical and experimental models. Appl Acoust 2003;64(6):611-632.
15. Zhou J, Bhaskar A, Zhang X. The effect of external mean flow on sound transmission through double-walled cylindrical shells lined with poroelastic material. J Sound Vib 2014;333:1972-1990.
16. Magniez J. Hamdi MA, Chazot JD, Troclet B. A mixed "Biot-Shell" analytical model for the prediction of sound transmission through a sandwich cylinder with a poroelastic core. J Sound Vib 2016;360:203-223.
17. Golzari M, Jafari AA. Sound transmission loss through triple-walled cylindrical shells with porous layers. J Acoust Soc Am 2018;143:3529-3544.
18. Vipperman JS, Li D, Avdeev I, Lane SA. Investigation of the sound transmission into an advanced grid-stiffened structure. J Vib Acoust 2003;125:257-266.
19. Rao SS. Vibration of Continuous Systems, New Jersey, USA. John Wiley & Sons; 2007.